Oncogene (2012) 31, 1408–1418

www.nature.com/onc

Open

ORIGINAL ARTICLE

Antitumor activity of a small-molecule inhibitor of the histone kinase Haspin

D Huertas[1], M Soler[1], J Moreto[1], A Villanueva[2], A Martinez[3], A Vidal[4], M Charlton[5], D Moffat[5], S Patel[5], J McDermott[5], J Owen[5], D Brotherton[5], D Krige[5], S Cuthill[5] and M Esteller[1,6,7]

[1]Cancer Epigenetics and Biology Program (PEBC), Bellvitge Biomedical Research Institute (IDIBELL), Barcelona, Catalonia, Spain; [2]Translational Research Laboratory, Institut Catala d'Oncologia, Bellvitge Biomedical Research Institute (IDIBELL), Barcelona, Catalonia, Spain; [3]Oncology Area, Center for Biomedical Research of La Rioja (CIBIR), Logroño, Spain; [4]Department of Pathology, Hospital Universitari de Bellvitge-IDIBELL, L'Hospitalet de Llobregat, Barcelona, Catalonia, Spain; [5]Chroma Therapeutics, Abingdon, Oxfordshire, UK; [6]Department of Physiological Sciences II, School of Medicine, University of Barcelona, Barcelona, Catalonia, Spain and [7]Institucio Catalana de Recerca i Estudis Avançats (ICREA), Barcelona, Catalonia, Spain

The approval of histone deacetylase inhibitors for treatment of lymphoma subtypes has positioned histone modifications as potential targets for the development of new classes of anticancer drugs. Histones also undergo phosphorylation events, and Haspin is a protein kinase the only known target of which is phosphorylation of histone H3 at Thr3 residue (H3T3ph), which is necessary for mitosis progression. Mitotic kinases can be blocked by small drugs and several clinical trials are underway with these agents. As occurs with Aurora kinase inhibitors, Haspin might be an optimal candidate for the pharmacological development of these compounds. A high-throughput screening for Haspin inhibitors identified the CHR-6494 compound as being one promising such agent. We demonstrate that CHR-6494 reduces H3T3ph levels in a dose-dependent manner and causes a mitotic catastrophe characterized by metaphase misalignment, spindle abnormalities and centrosome amplification. From the cellular standpoint, the identified small-molecule Haspin inhibitor causes arrest in G2/M and subsequently apoptosis. Importantly, *ex vivo* assays also demonstrate its anti-angiogenetic features; *in vivo*, it shows antitumor potential in xenografted nude mice without any observed toxicity. Thus, CHR-6494 is a first-in-class Haspin inhibitor with a wide spectrum of anticancer effects that merits further preclinical research as a new member of the family of mitotic kinase inhibitors.
Oncogene (2012) **31,** 1408–1418; doi:10.1038/onc.2011.335; published online 1 August 2011

Keywords: epigenetics; histone; inhibitor

Correspondence: Dr M Esteller, Cancer Epigenetics and Biology Program (PEBC), Bellvitge Biomedical Research Institute (IDIBELL), Third Floor, Hospital Duran i Reynals, Avda. Gran Via de L'Hospitalet 199-203, L'Hospitalet-08908, Barcelona, Catalonia, Spain.
E-mail: mesteller@idibell.cat
Received 19 January 2011; revised 23 May 2011; accepted 28 June 2011; published online 1 August 2011

Introduction

The initiation and progression of cancer are now assumed to involve not only genetic alterations but also disruption of epigenetic patterns (Jones and Baylin, 2007; Berdasco and Esteller, 2010). The cancer epigenome is characterized by characteristic changes in DNA methylation and histone modification patterns (Jones and Baylin, 2007; Berdasco and Esteller, 2010). Unlike genetic mutations, DNA methylation and histone modification marks are potentially reversible by the use of drugs that target the epigenetic enzymes (Jones and Baylin, 2007; Berdasco and Esteller, 2010). In this regard, inhibitors of histone deacetylases and DNA-demethylating agents have been developed and approved for use in the therapy of hematological malignancies, such as cutaneous T-cell lymphoma (Lane and Chabner, 2009; Marks, 2010) and myelodysplastic syndrome (Bryan *et al*., 2010; Götze *et al*., 2010), respectively. However, these drugs have so far shown limited activity against solid epithelial tumors (Graham *et al*., 2009; Ma *et al*., 2009). Thus, it is necessary to search for new drugs and pathways that target the epigenetic machinery and might therefore be useful for treating a wide spectrum of human tumors.

An interesting possibility is the discovery of compounds that target histone phosphorylation, a post-translational modification of these proteins that is involved in mitotic functions, particularly in the phosphorylation of serine 10 (H3S10ph) and threonines 3 (H3T3ph) and 11 (H3T11ph) of histone H3 (Kouzarides, 2007). Kinases can be blocked by small molecules and, recently, mitotic kinases such as Cdks (cyclin-dependent kinases) (Vassilev *et al*., 2006; Malumbres *et al*., 2008), Polo-like-kinases (Johnson *et al*., 2007; Gleixner *et al*., 2010) and Aurora kinases (Harrington *et al*., 2004; Girdler *et al*., 2006) have been studied as potential targets for cancer therapy with fewer side effects than traditional cytotoxic drugs. The case of Aurora kinase B is particularly interesting because this enzyme phosphorylates H3Ser10 and is associated with microtubules during chromosome movement and segregation. Importantly, Aurora kinase B inhibitors are

under study in several clinical trials (Dar *et al*., 2010). Thus, in a similar manner, we concentrated our efforts on developing small-molecule inhibitors of another enzyme that phosphorylates histones, Haspin (Haploid Germ Cell-Specific Nuclear Protein Kinase) (Dai *et al*., 2005; Dai *et al*., 2006; Dai *et al*., 2009).

Haspin is a kinase that specifically phosphorylates histone H3 at threonine 3 (H3T3ph) (Dai *et al*., 2005, 2006, 2009). Haspin function is critical in mitosis, favoring chromosome cohesion, metaphase alignment and progression though the cell cycle (Dai *et al*., 2005, 2006, 2009). These properties lead us to consider that inhibitors of Haspin can be efficient anti-mitotic compounds. In addition, inhibition of Haspin might have fewer undesirable side effects than other drug-targeted mitotic kinases because it belongs to a protein kinase family that diverges from other human kinases (Higgins, 2001; Eswaran *et al*., 2009; Villa *et al*., 2009) and it has only one known target: H3T3 phosphorylation (Dai *et al*., 2005; Dai *et al*., 2006; Dai *et al*., 2009). As with other mitotic kinases, its function is related to proliferating cells, and we expect that inhibitor compounds will not affect non-proliferating cells. The first small-molecule inhibitors of Haspin have recently been identified by high-throughput screening using a homogeneous time-resolved fluorescence resonance energy transfer (FRET) assay, but *in vivo* assays have not been performed (Patnaik *et al*., 2008; Cuny *et al*., 2010). Herein, we describe a new small-molecule inhibitor of Haspin, CHR-6494, with powerful antitumoral activity *in vitro*, *ex vivo* and *in vivo*.

Results

Library screening for Haspin inhibitors

An initial high-throughput radiometric enzymatic Haspin kinase assay based on the incorporation of radioactivity from [γ-33P]-ATP into histone H3 in a homogeneous FlashPlate 384-well format (Invitrogen, Paisley, UK) using a library of 117 995 compounds screened at 10 μM was developed (BioFocus DPI, Allschwill, Switzerland). A total of 1271 compounds from the screening (having >50% inhibition) were retested in duplicate and 591 showed confirmed activity. Cluster and physical property analyses of these hits highlighted 125 compounds as being suitable for IC_{50} evaluation and purity analysis. On the basis of dose-response results and molecular similarity studies, a further 456 compounds were identified from the BioFocus DPI compound collection and commercial sources for hit expansion IC_{50}, and liquid chromatography and mass spectrometry purity measurements. From the results for compounds with a purity >70%, 123 compounds were identified with an IC_{50} <10 μM. Several hit series were identified in this exercise and three were selected for hit-to-lead studies. Two of these series, while maintaining Haspin kinase inhibition, performed poorly in cell-based assays; hence, a series of imidazopyridazines were chosen for further optimization. CHR-6494 (3-(1H-indazol-5-yl)-*N*-propylimidazo[1,2-b]pyridazin-6-amine) (Figure 1a) was identified as a compound having promising Haspin kinase and cell proliferation-inhibitory properties that merited further detailed biological and antitumor investigation.

CHR-6494 is a potent inhibitor of histone H3T3 phosphorylation that has anti-proliferative effects in human cancer cells

The next step was to show that the CHR-6494 compound was indeed an active Haspin inhibitor with important biological effects, such as inhibition of cell proliferation. To this end, we chose the initial biological model of human cancer cell lines, in which three of the best recognized examples, namely HeLa (cervical), HCT-116 (colon) and MDA-MB-231 (breast) were selected. CHR-6494 inhibited histone H3T3 phosphorylation in the three cancer cell lines in a dose-dependent manner as shown by western blot (Figure 1b) and immunofluorescence (Figure 1c). The diminished H3T3 phosphorylation levels upon CHR-6494 treatment were not associated with downregulation of the total content of the Haspin protein, the enzyme targeted by the drug (Figure 1d). The use of CHR-6494 did not modify H3S10 and H328 phosphorylation levels (Figure 1d), two sites that are not phosphorylated by Haspin, emphasizing the enzyme specificity of the identified inhibitor. The specificity of CHR-6494 for Haspin was further confirmed by analysis of the enzymatic inhibitory capacity of the compound in a panel of 27 protein kinases, including Aurora B kinase. Using a FRET assay based on the differential sensitivity of phosphorylated and non-phosphorylated peptides to protein cleavage (Z′-LYTE Kinase Assay, Invitrogen), we observed that the IC_{50} value for Haspin was 2 nM, whereas for all other protein kinases, it was in the μM range (Supplementary Table 1).

Once the biochemical effects of CHR-6494 as a Haspin inhibitor had been confirmed, we assessed its effect on cancer cell biology. Using the XTT ((2,3-bis-(2-methoxy-4-nitro-5-sulfophenyl)-2H-tetrazolium-5-carboxanilide)) assay to measure cell viability in the three described cancer cell lines, we observed that CHR-6494 inhibited cancer cell growth dose dependently (Figure 2a). The IC_{50} values were within the same range: 500 nM for HCT-116, 473 nM for HeLa and 752 nM for MDA-MB-231. Interestingly, IC_{50} sensitivity to this first-in-class Haspin inhibitor compound is in the same range as that of other anticancer compounds that target histone modifications, such as inhibitors of Aurora kinases A and B (Carpinelli and Moll, 2008) and histone deacetylase (Zubia *et al*., 2009). The IC_{50} values upon CHR-6494 treatment for the Wi-38 human diploid cell line derived from normal embryonic lung tissues doubled those obtained for cancer cells (IC_{50} = 1059 nM) (Supplementary Figure 1), highlighting a higher cell-viability effect on cancer cells rather than on just proliferating cells. To further show that the effect on cell viability of the drug was mediated by the inhibition of Haspin, we overexpressed the protein in HeLa cells and observed a partial rescue from the effects

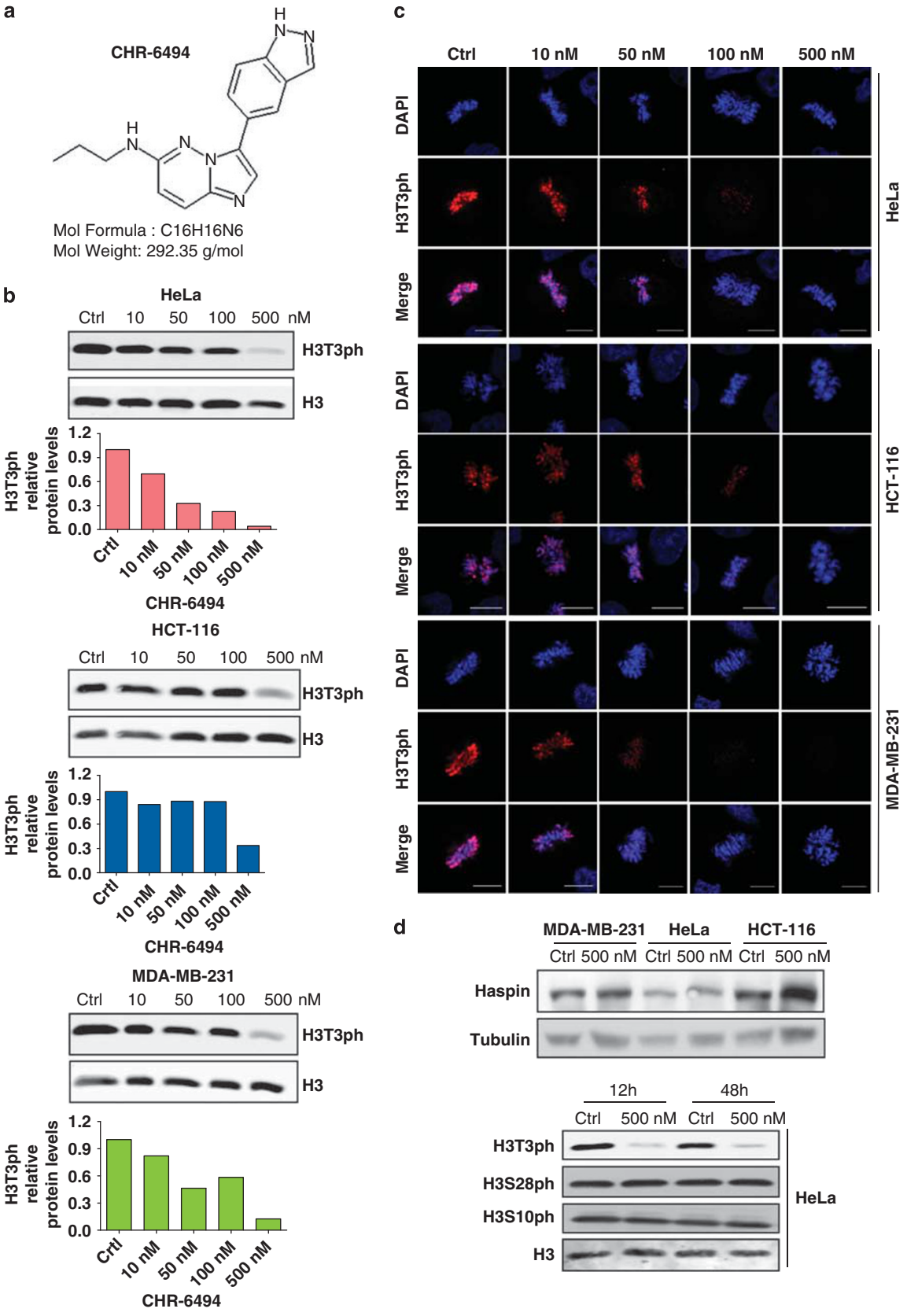
a
CHR-6494
Mol Formula : C16H16N6
Mol Weight: 292.35 g/mol
b
HeLa
Ctrl 10 50 100 500 nM
H3T3ph
H3
H3T3ph relative protein levels
1.2
0.9
0.6
0.3
0.0
Crtl
10 nM
50 nM
100 nM
500 nM
CHR-6494
HCT-116
Ctrl 10 50 100 500 nM
H3T3ph
H3
H3T3ph relative protein levels
CHR-6494
MDA-MB-231
Ctrl 10 50 100 500 nM
H3T3ph
H3
H3T3ph relative protein levels
CHR-6494
c
Ctrl
10 nM
50 nM
100 nM
500 nM
DAPI
H3T3ph
Merge
HeLa
HCT-116
MDA-MB-231
d
MDA-MB-231
HeLa
HCT-116
Ctrl 500 nM Ctrl 500 nM Ctrl 500 nM
Haspin
Tubulin
12h
48h
Ctrl 500 nM Ctrl 500 nM
H3T3ph
H3S28ph
H3S10ph
H3
HeLa

of the compound: Haspin-transfected HeLa cells had an increased IC_{50} value in comparison with control HeLa cells (Supplementary Figure 2).

The described inhibition of cell proliferation induced by CHR-6494 was associated with the induction of cell-cycle arrest at G2/M in a dose-dependent manner (Figure 2b) and subsequent apoptosis (Figure 2c). The cell cycle was assessed with propidium iodide (PI)-stained cells (distribution of cells in G_0/G_1, S and G_2/M phases) by flow cytometry. Annexin V-fluorescein isothiocyanate/PI double staining was used to detect cell apoptosis. Upon CHR-6494 administration, the basal 8–15% of cells in G_2/M observed in carrier control (dimethyl sulfoxide (DMSO))-treated cells increased to 30–50% (Figure 2b), indicating that progression through mitosis was delayed. Upon withdrawal of CHR-6494 treatment for 24 and 48 h, the HCT-116 line retained 50% of cells in G2/M arrest, suggesting a prolonged effect of the drug. Related to the induction of programmed cell death, if the vast majority of cells from the three studied lines were alive upon carrier treatment, the use of CHR-6494 induced the entrance of these cells into apoptosis with incorporation of Annexin V (Figure 2c). The apoptotic effect ranged from 89.88 and 63.27% in HeLa and HCT-116, respectively, to 30.41% in MDA-MB-231 cells.

The inhibition of histone H3T3 phosphorylation induced by CHR-6494 causes a mitotic catastrophe

The knowledge that phosphorylation of H3T3 by Haspin is required for correct chromatid cohesion and metaphase alignment (Dai *et al*, 2005; Dai *et al*. 2006; Dai *et al*. 2009), and our finding that the Haspin inhibitor blocks normal progression through the cell cycle, led us to consider the effects of possible mitotic spindle and centrosome defects upon CHR-6494 treatment. Immunofluorescence data had already confirmed that, in control-treated cells, the H3T3ph signal is

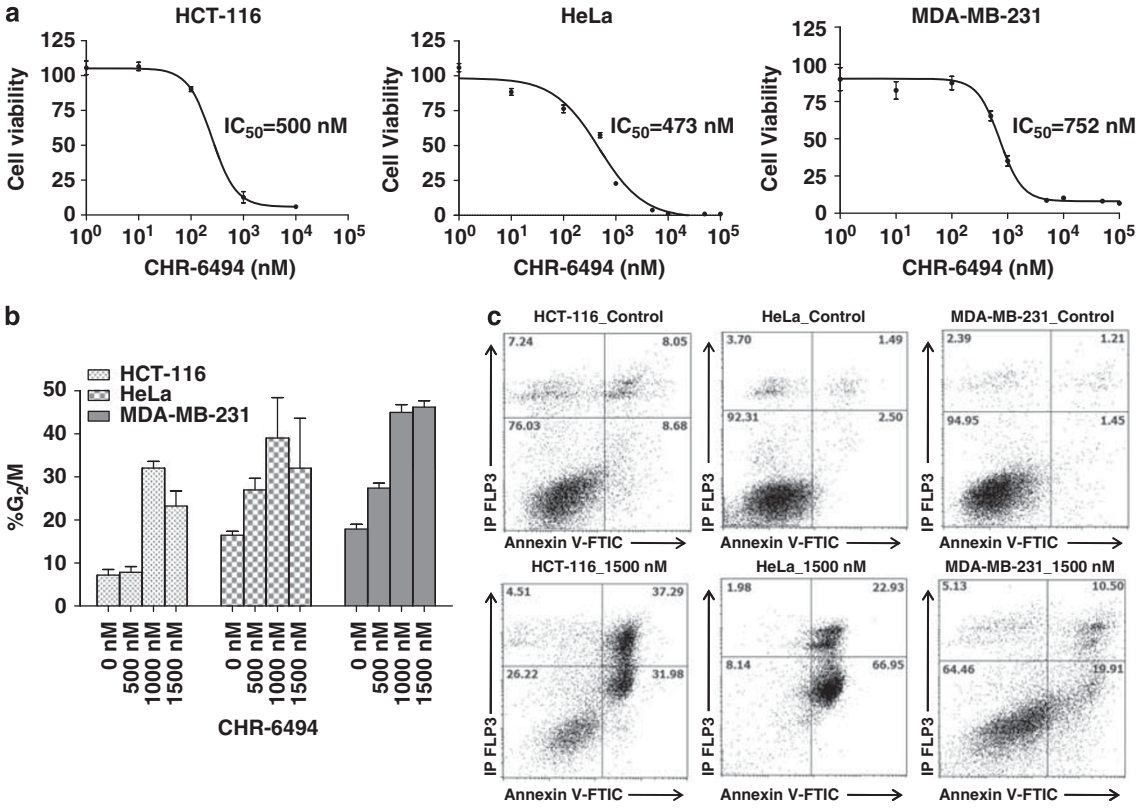

Figure 2 CHR-6494 treatment decreases cell viability, causes an arrest in G2/M and later apoptosis. (**a**) Effect of CHR-6494 in cell viability determined by the XTT assay in HCT-116, HeLa and MDA-MB-231 cells. IC_{50} values are shown for each cell line. (**b**) Effect of CHR-6494 in the cell cycle. The percentage of G_2/M cells is CHR-6494 dose dependent, indicating that progression through mitosis is delayed. (**c**) The proapoptotic effect of CHR-6494. Upon Haspin inhibitor use, the percentage of cell death increases in the three cancer cell lines, as demonstrated by incorporation of Annexin V.

Figure 1 CHR-6494 is a small-molecule inhibitor of Haspin. (**a**) Chemical structure of CHR-6494. (**b**) H3T3ph levels in human cancer cell lines upon CHR-6494 treatment determined by western blot quantified using the Odyssey IR scanner. (**c**) H3T3ph immunofluorescence signal in mitotic chromosomes of HeLa, HCT-116 and MDA-MB-231 cells upon CHR-6494 use. In both panels **b** and **c**, the H3T3ph mark is extremely low at 500 nM concentration of the drug. Scale bar is 10 μm. (**d**) The use of the Haspin inhibitor does not affect the global levels of the enzyme (top). CHR-6494 does not change the phosphorylation levels of other residues of histone H3 not catalyzed by Haspin (H3S28ph and H3S10ph) (below). Total H3 is used as a loading control.

present in the chromosomes of mitotic cells, a mark that decreased in a dose-dependent manner upon CHR-6494 treatment (Figure 1c). However, the use of the Haspin inhibitor also had an important effect on the morphology of mitotic spindle and centrosome structure of cancer-treated cells. Immunofluorescence assays with anti-α-tubulin showed that control cells displayed normal bipolar mitotic spindles with chromosomes correctly aligned along the metaphase plate in the three cancer cell lines (Figure 3a). On the other hand, CHR-6494-treated cells exhibited an abnormal mitotic spindle with large defects in chromosomal alignment, such as the existence of multi-polar spindle morphology in the three cancer cell lines (Figure 3a). Cells displaying aberrant spindles did not progress through the anaphase, and the percentage of cells in the anaphase decreased in a CHR-6494 dose-dependent manner (Figure 3b).

The abnormal spindles observed upon CHR-6494 treatment might have been a consequence of defects in centrosome duplication (Thompson *et al*., 2010). Thus, we analyzed the number of centrosomes in HeLa, HCT-116 and MDA-MB-231 cells by immunostaining with anti-γ-tubulin, a protein localized in the centrosomes, combined with histone H3S10ph staining, a marker of mitosis (Figure 3c). We observed that carrier-treated cells had two centrosomes in every stage of the mitotic cell cycle in the three studied lines (Figure 3c). However, the number of centrosomes increased with the use of increasing concentrations of the Haspin inhibitor (Figure 3c). To confirm that the observed centrosome amplification was not an effect of centrosome reorganization due to aberrant spindle configuration, we calculated the number of centrosomes in the prophase just before spindle formation (Figure 3d). Treatment with the Haspin inhibitor also increased the number of centrosomes in the prophase (Figure 3d). Thus, CHR-6494 caused an abnormal duplication of centrosomes that it is dose dependent.

In addition to centrosome amplification, the chromosomes of CHR-6494-treated cells had other important aberrant structures in the metaphase and anaphase, such as wider chromatids (Figures 1c, 3a and 3b), which were probably associated with defects in condensation and/or cohesion. There are several checkpoint controls that function to safeguard the genome by limiting progression until events have been properly concluded and, for example, the spindle checkpoint proteins (such as Mad1,

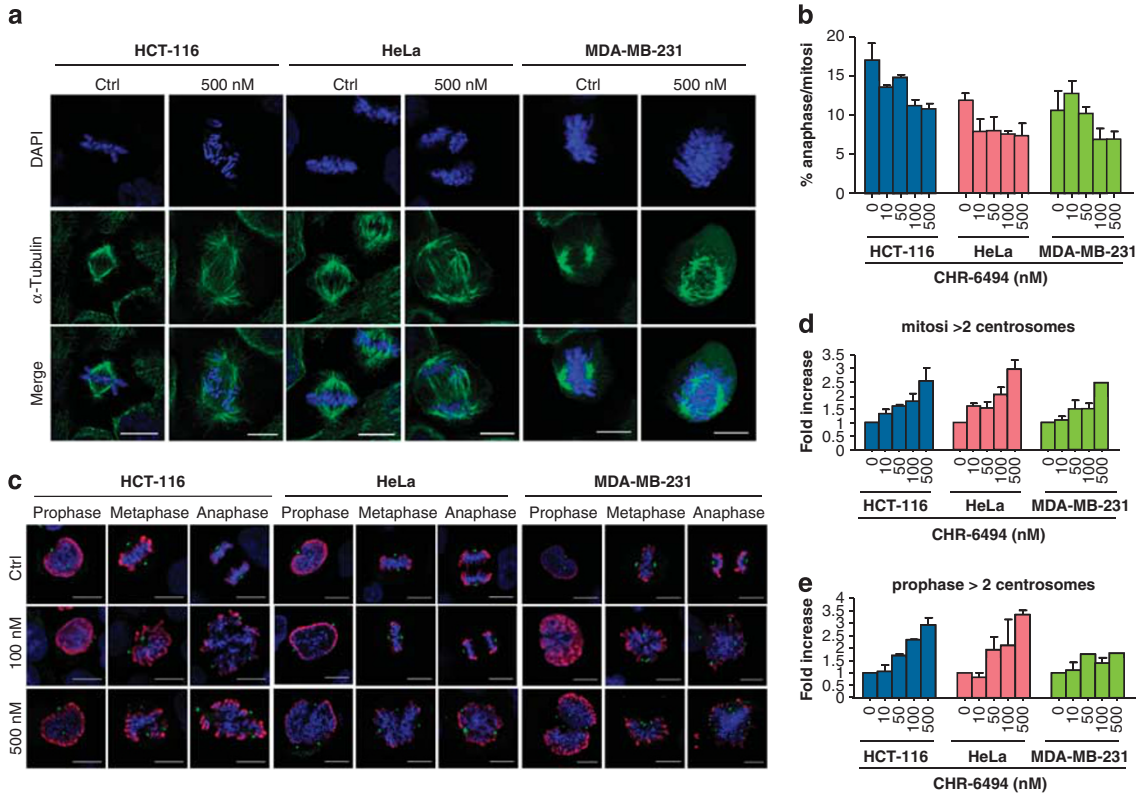

Figure 3 CHR-6494 treatment causes a mitotic catastrophe with abnormal morphology of the mitotic spindle and centrosome amplification. (**a**) Immunostaining of mitotic spindle with anti α-tubulin in control and CHR-6494-treated cells. (**b**) The percentage of anaphase in mitotic cells treated with CHR-6494 is dose dependent. (**c**) Immunostaining of centrosomes with anti γ-tubulin in mitotic cells treated with CHR-6494. Mitotic cells have been localized by immunostaining with the H3S10ph antibody (red staining) and marked with anti γ-tubulin (green dots), and chromosomes are labeled with DAPI in the blue channel. (**d**) The percentage of cells with more than two centrosomes in every mitosis after treatment with CHR-6494 increases up to three at higher concentrations of CHR-6494. (**e**) The percentage of cells with more than two centrosomes per prophase after treatment with CHR-6494 is also dose dependent, indicating that spindle defects are probably a consequence of centrosome amplification. The images showed in this figure are the result of the maximum *Z*-projection of 6–10 stacks, taken every 1 μm. Scale bar is 10 μm.

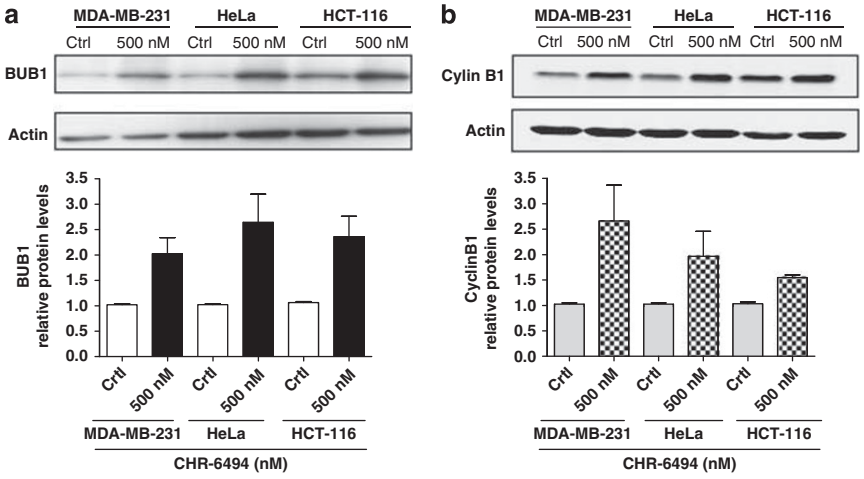

Figure 4 CHR-6494 treatment upregulates the spindle assembly checkpoint protein BUB1 (**a**) and the marker of mitotic arrest cyclin B1. (**b**) Western blots and quantification of the levels of cyclin B1 and BUB1 are shown in control and CHR-6494-treated cells.

Mad2, BUB1, Bub3 and BubR1) examine the alignment and tension of chromosomes in the mitotic spindle before initiation of the anaphase (Musacchio and Salmon, 2007). These mitotic spindle checkpoint proteins might arrest cells in the metaphase by suppressing Cdc20, a protein required to trigger ubiquitination and consequent degradation of cyclin B (Nilsson *et al*., 2008). This degradation allows separase activation, which triggers the separation of sister chromatids (Stemmann *et al*., 2006). To investigate whether Haspin inhibition by the CHR-6494 compound also caused misregulation of checkpoints, we analyzed the levels and nuclear localization of the key spindle assembly checkpoint protein BUB1 and the marker of mitotic arrest cyclin B1. Western blot experiments demonstrated that BUB1 and cyclin B1 were both upregulated in the three cancer cell lines upon CHR-6494 treatment (Figure 4). These results indicate that the mitotic spindle checkpoint mediated by BUB1 undergoes activation before progression to the anaphase to try to correct the aberrant spindle caused by the Haspin inhibitor. This event is followed by an arrest in G_2/M (Figure 2b) and marked by the observed upregulation of cyclin B1 levels.

CHR-6494 inhibits angiogenesis ex vivo *and tumor growth in xenografted mice*

The current development of efficient anticancer drugs must take into account all the crucial steps in tumor development and metastasis, among them the targeting of new blood vessel formation (Folkman, 2007). In this regard, other epigenetic drugs such as histone deacetylase inhibitors have shown anti-angiogenic potential (Kim *et al*., 2001; Aizpea *et al*., 2009), although this has yet to be fully explored. Thus, we speculated whether the newly identified Haspin inhibitor could act as a blocking agent against angiogenesis. We found that CHR-6494 was an inhibitor of angiogenesis in the *ex vivo* chicken embryo aortic arch ring assay (Figure 5a). At a concentration of 1 μM CHR-6494, there is a 70% reduction of the sprouting vessel area induced by the pro-angiogenic basic Fibroblast Growth Factor (bFGF). Thus, the identified Haspin inhibitor, in addition to its anti-proliferative and proapoptotic features, has an anti-angiogenic capacity that could be useful for therapeutic purposes.

We transferred our experiments from the *in vitro* and *ex vivo* assays described above to the *in vivo* setting in a mouse model. The antitumor activity of CHR-6494 was evaluated using HCT-116 human colorectal cancer cells xenografted in nude mice. Dose-dependent tumor growth inhibition was demonstrated upon subcutaneous administration of CHR-6494 (Figure 5b). Interestingly, if we ceased administration of the Haspin inhibitor, the tumor started to regrow (Figure 5b), demonstrating that the anti-proliferative effect was caused by the presence of CHR-6494. Histopathological analyses revealed no abnormality in any of the normal mouse tissues studied (Figure 5c), and the body weight of CHR-6494-treated mice did not change during the treatment period (Figure 5d), implying the lack of toxicity of the drug under the described conditions.

Overall, our results indicate that the CHR-6494 compound is a first-in-class Haspin inhibitor that blocks H3T3ph, causing mitotic spindle and centrosome defects that are associated with an arrest in G_2/M and subsequent apoptosis, in addition to demonstrating *ex vivo* anti-angiogenesis and *in vivo* antitumoral effects. Thus, CHR-6494 can be considered to be a new candidate compound that warrants further development for use in epigenetic cancer therapy.

Discussion

The CHR-6494 compound can be considered a first-in-class inhibitor of the histone kinase Haspin that has been characterized *in vitro* and *in vivo*. Only one report has previously described other potential inhibitors of Haspin that were identified in high-throughput *in vitro* screening using an enzymatic assay (Patnaik *et al*., 2008; Cuny *et al*., 2010). Herein, starting from a library of 117 995 compounds, we have comprehensively characterized the CHR-6494 small molecule as a specific

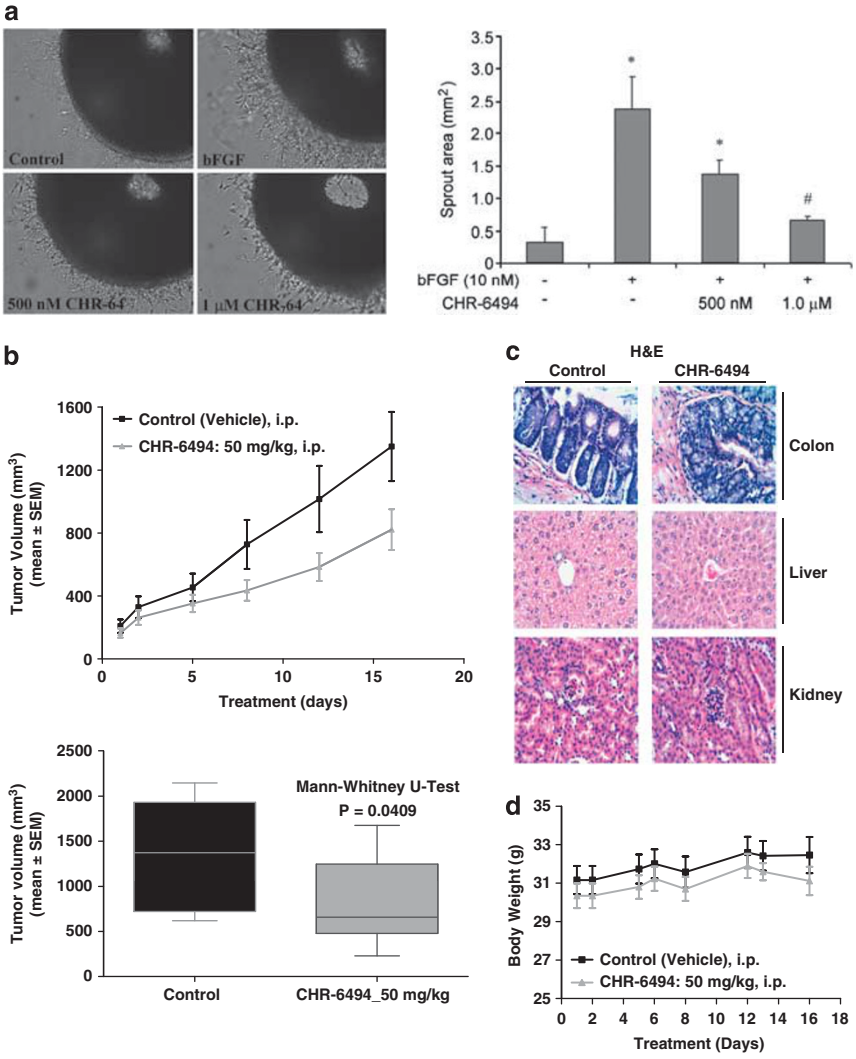

Figure 5 CHR-6494 treatment inhibits *ex vivo* angiogenesis and *in vivo* tumor growth in xenografted nude mice. (**a**) Left, photographs of chicken embryo aortic arch ring embedded in synthetic matrix and exposed to the pro-angiogenic bFGF alone or in combination with CHR-6494 (500 nM and 1 μM); right, quantification of the sprout number decreases upon Haspin inhibitor treatment (Kruskal–Wallis followed by a Mann–Whitney *post hoc* test). (**b**) Antitumoral activity of CHR-6494 in HCT-116 xenografts in nude mice. Top, tumor volume is monitored over time in mock- and CHR-6494-treated mice. Below, graphical plots at the time of killing of animals at 16 days demonstrate tumor volume reduction upon Haspin inhibitor treatment (Mann–Whitney *U*-test). (**c**) Hematoxylin–eosin staining of colon, liver and kidney sections of nude mice upon CHR-6494 treatment did not show evidence of toxicity. (**d**) Graph measuring the weight of mice upon treatment: the body weight of CHR-6494-treated mice did not change during the treatment period.

Haspin inhibitor that blocks H3T3 phosphorylation in association with a characteristic spindle and centrosome phenotype, causes arrest in G2/M, induces apoptosis and possesses *ex vivo* anti-angiogenesis features and antitumoral properties in a xenografted nude mice model. These results might be relevant in at least two ways: by improving our knowledge of the biology and functions of the Haspin protein; and by providing opportunities for carrying out further studies of the safety and efficacy of the compound in a preclinical setting for future clinical trials in cancer therapy.

From the biochemical and cell biological standpoint, the discovery of a specific Haspin inhibitor such as CHR-6494 might enable its use as a powerful experimental tool with which we can understand the activities of this protein. Haspin is a protein kinase conserved in eukaryotes, where it associates with chromosomes in mitosis, preferentially at the centromeres (Dai *et al*., 2005, 2009, 2006). Haspin is required for phosphorylation of H3T3 to ensure proper chromatid cohesion and metaphase alignment and for normal progression through the cell cycle (Dai *et al*., 2005, 2009, 2006). It has also been proposed that Haspin phosphorylation of H3T3 at the centromere facilitates Aurora B activation (Rosasco-Nitcher *et al*, 2008). Very recently, the mechanism of Haspin action has been revealed in three studies showing that histone H3T3 phosphorylation is a requisite for Aurora B, as it is positioned at the centromeres in mitosis, and that Survivin, a member of the chromosomal passenger complex, binds directly to

H3T3ph (Wang *et al*., 2010, Kelly *et al*., 2010). In addition, it has been shown that H3T3 phosphorylation cooperates with BUB1-mediated H2AS121 phosphorylation in targeting the chromosomal passenger complex to the inner centromere to facilitate chromosome bi-orientation (Yamagishi *et al*., 2010). We discovered that the loss of H3T3ph by CHR-6494-associated inhibition of Haspin causes metaphase misalignment, spindle and centrosome defects, as well as BUB1 and cyclin B1 upregulation, which mimics the phenotypes already described using RNA interference against Haspin (Dai *et al*., 2005, 2006, 2009). These results indicate that CHR-6494 is a useful tool for learning about the physiological role of Haspin and avoids problems associated with the use of RNA interference to understand its role in tumorigenesis.

For the future development of Haspin inhibitors in the clinical arena, we show herein that CHR-6494 has a mechanism of action similar to that of other developed inhibitors of mitotic kinases, such as Aurora A and Aurora B kinases (Dar *et al*., 2010) or Polo-like kinase (Macurek *et al*., 2009; Gleixner *et al*., 2010; Chopra *et al*., 2010): the phenotype in mitosis is associated with cessation of cell proliferation, G_2/M cell-cycle arrest, activation of spindle checkpoint proteins such as BUB1 and induction of apoptosis. However, the mitotic catastrophe phenotype achieved by these drugs is not identical. One example is that Aurora B kinase inhibitors increase the polyploidy level due to endoreplication and the absence of cytokinesis (D'Alise *et al*., 2008; Oke *et al*., 2009; Tao *et al*., 2009), which we did not observe in CHR-6494-treated cells. Interestingly, the IC_{50} concentration of CHR-6494 is in the range of 0.5–1.0 μM, which is also similar to that observed in the aforementioned cell proliferation inhibitors. Therefore, CHR-6494 is a member of the new generation of anti-mitotic compounds that target components of the mitotic machinery other than microtubules. Thus, CHR-6494 avoids some of the adverse effects associated with taxanes, which block cell-cycle progression by binding to tubulin, causing undesirable cytotoxic effects arising because of tubulin's role as a cytoskeletal protein that is essential for many other cell functions in addition to mitosis. This new generation of anti-mitotic drugs also targets centrosomes, like the compound K858, which inhibits the mitotic kinesin Eg5 causing mitotic arrest, monopolar spindles and monocentrosomes (Nakai *et al*., 2009), Griseofulvin, which inhibits centrosomal clustering (Rebacz *et al*., 2007) and Fostriecin, which inhibits the phosphatase PP2A and induces centrosome replication and aberrant mitotic spindles (Cheng *et al*., 1998, Takeuchi *et al*., 2009), as well as the inhibitors of Polo-like kinases (Chopra *et al*., 2010) and Aurora A kinase (Dar *et al*., 2010).

Overall, our data suggest that CHR-6494 is a specific inhibitor of the histone kinase Haspin that causes a mitotic catastrophe in cancer cells, which explains its significant antitumor activity in the various experimental layers that we have assessed. Other mitotic kinase inhibitors are already under clinical trial (Dar *et al*., 2010) and the Haspin protein is overexpressed in lymphomas (Rosenwald *et al*., 2001; Dave *et al*., 2006); hence, further studies about bioavailability, pharmacokinetics, dose administration and additional cellular and animal models of cancer are warranted for the preclinical development of CHR-6494 to evaluate the potential of the compound as an anticancer drug.

Materials and methods

Library screening for Haspin inhibitors

A high-throughput radiometric enzymatic Haspin kinase assay based on the incorporation of radioactivity from [γ-33P]-ATP into histone H3 in a homogeneous FlashPlate 384-well format (Invitrogen) was used. In brief, 10 μl of compound in the assay buffer was mixed with 20 μl Haspin enzyme (10 ng per well) and histone H3 substrate (1.5 μg per well) and the reaction started by the addition of 20 μl [γ-33P]-ATP. After 75 min of incubation at room temperature (RT), the reaction was stopped by the addition of EDTA (final concentration 33 mM). Wells were washed three times with 80 μl assay buffer, and plates then sealed and counted in a TopCount Counter (TopCount Counter, Meriden, CT, USA) for 30 s per well.

Cell culture

HeLa (human cervical carcinoma cell line), HCT-116 (human colon carcinoma cell line) and MDA-MB-231 (human breast cancer cell line) were obtained from ATCC (American Type Culture Collection, ATCC, Manassas, VA, USA) and cultured in Dulbecco's modified Eagle's medium (PAA Laboratories GmbH, Pasching, Austria) containing stable glutamine, and supplemented with 10% heat-inactivated fetal bovine serum (Invitrogen) and 1% penicillin–streptomycin (both antibiotics, PAA Laboratories GmbH). Cells were grown at 37 °C in a humidified atmosphere of 5% CO_2 and 95% air. For transfection assays, pCMV6-XL5 (SC 314727, NM-031965.2-True Clone cDNA Clone) was used for Haspin expression (Origene, Rockville, MD, USA). In brief, cells were transfected using Lipofectamine 2000 (Invitrogen) according to the manufacturer; 90–95% confluent cells were transfected with 2 μg of DNA vector in Opti-MEM I Reduced Serum Medium (Invitrogen) mixed with Lipofectamine, and cells were incubated at 37 °C in a CO_2 incubator for 18–48 h before testing for transgene expression by western blot.

Drug, cell viability and kinase assays

CHR-6494 (Chroma Therapeutics, Oxfordshire, UK) was supplied as a powder and dissolved at 10 mM in DMSO and stored at −20 °C (10 mM stock). Cells were treated for 24, 48 and 72 h with the inhibitor or with DMSO as a control. Cell viability was assessed using the colorimetric XTT assay (Roche Diagnostics GmbH, Mannheim, Germany) according to the manufacturer's protocol. Cells were seeded in 94-well plates (SPL Lifescience, Gyeonggi, Korea) at a density of 4×10^4 cells per well, and allowed to attach for 24 h. The medium was then exchanged with others containing different drug concentrations (0.001−10 μM). Eight wells for each concentration of the CHR-6494 compound were used. At the corresponding time, the culture medium was discharged, the XTT reagent was added and the final cell number and optical density were determined. Dose-response curves were generated and cell viability was evaluated after 72 h of treatment. The half-maximal inhibitory concentration (IC_{50}) was determined using GraphPad Prism (GraphPad, San Diego, CA, USA) software. The analysis of the enzymatic inhibitory capacity of the

compound in a panel of 29 protein kinases was developed using a FRET assay based on the differential sensitivity of phosphorylated and non-phosphorylated peptides to protein cleavage (Z′-LYTE Kinase Assay, Invitrogen). In the primary reaction, the kinase transfers the γ-phosphate of ATP to a single tyrosine, serine or threonine residue in a synthetic FRET peptide. In the secondary reaction, a site-specific protease recognizes and cleaves non-phosphorylated FRET peptides. Phosphorylation of FRET peptides suppresses cleavage by the development reagent. Cleavage disrupts FRET between the donor (that is, coumarin) and the acceptor (that is, fluorescein) fluorophores on the FRET peptide, whereas uncleaved, phosphorylated FRET peptides maintain FRET. A ratiometric method, which calculates the ratio (the emission ratio) of donor emission to acceptor emission after excitation of the donor fluorophore at 400 nM, is used to quantitate reaction progress.

Apoptosis and cell-cycle analysis

Cells were seeded in 150-mm plastic culture dishes (SPL Lifescience) at a density of 2.5×10^6 for HCT-116 and HeLa cells, and 3.5×10^6 for the MDA-MB-231 cell line, and allowed to attach for 24 h. The medium was then exchanged with others containing different drug concentrations (0.5, 1, 1.5 μM) or with DMSO as a control. After 48 h, floating and attached cells were collected, and washed with phosphate-buffered saline (PBS). Annexin V-fluorescein isothiocyanate/PI double staining (BD Pharmingen, San Diego, CA, USA) was used to detect cell apoptosis according to the manufacturer's instructions. Approximately 2.5×10^5 cells were resuspended in 250 μl of binding buffer and 5 μl of Annexin V-fluorescein isothiocyanate. After a 10-min incubation at RT in the dark, cells were washed, resuspended in 400 μl binding buffer and stained with 1 μg/ml of PI. Positivity for Annexin V-fluorescein isothiocyanate and/or PI was analyzed using a FACS flow cytometer (FACSCalibur, Becton Dickinson, Franklin Lakes, NJ, USA). Data obtained from three experiments were collected and mean and s.d. of the percentage of apoptotic cells were calculated.

The cell cycle was assessed with PI-stained cells (distribution of cells in G_0/G_1, S and G_2/M phases) by flow cytometry. Approximately 2×10^6 cells were fixed in ice-cold 70% ethanol overnight at −20 °C. Cells were subsequently washed and resuspended in phosphate-citrate buffer. After 30 min, DNA was stained with 25 μg/ml PI (Sigma, St Louis, MO, USA) in a reaction solution containing 50 μg/ml RNAse A (Sigma) for 30 min at 37 °C in the dark. Fluorescence emitted from the PI–DNA was measured for individual cells using a FACS flow cytometer. Data from three experiments were collected and mean and s.d. of the percentage of cells in the G_2/M phase were calculated.

Western blot analysis of H3 phosphorylation, Haspin, cyclin B1 and BUB1 expression

HCT-116, HeLa and MDA-MB-231 cells were treated with 500 nM of CHR-6494 compound (or 0.1% DMSO as a control) for 48 h, and then harvested and washed twice with PBS. Finally, they were centrifuged at 400 *g* for 5 min. Cell pellets were resuspended in lysis buffer (10% glycerol, 2% SDS w/v, 63 mM Tris-HCl pH 6.8, 0.01% bromophenol blue, 2% 2-mercaptoethanol), sonicated and boiled for 5 min. Equal amounts of protein extracts were loaded onto Tris–Glycine-SDS gels, and transferred to a nitrocellulose membrane (Whatman, GE Healthcare, Chalfont St Giles, UK). Membranes were blocked with Odyssey blocking buffer (Li-COR, Lincoln, NE, USA), diluted 1:1 in tris-buffered saline (TBS) for 1 h at RT. Primary antibodies were diluted in Odyssey blocking buffer combined with 1:1 in TBS, containing 0.05% Tween-20 and incubated O/N at 4 °C. Final antibody concentrations were 1:5000 for H3T3ph (rabbit PAb, Millipore, Billerica, MA, USA), 1:4000 for H3 (mouse MAb, Abcam, Cambridge, UK), 1:500 for Haspin (rabbit PAb, Abcam); 1:6000 for H3S28 (rat MAb, Sigma-Aldrich, St Louis, MO, USA); 1:8000 for H3S10 (rabbit MAb, Upstate, Billerica, MA, USA), 1:10 000 for tubulin (rabbit PAb, Abcam), 1:2000 for cyclin B1 (mouse MAb, Cell Signaling, Danvers, MA, USA), 1:1000 for BUB1 (mouse MAb, Abcam) and 1:4000 for Actin (mouse MAb, Sigma-Aldrich). After primary antibody incubations, membranes were washed three times (10 min each) with TBS containing 0.05% Tween-20 at RT on a bench-top shaker. Secondary antibodies conjugated to IRDye 800CW (Li-COR) or IRDye 680 (Li-COR), and then diluted to a concentration of 1:20 000 in Odyssey blocking buffer combined 1:1 with TBS, containing 0.05% Tween-20. Membranes were incubated with secondary antibody solutions for 1 h at RT in the dark on a bench-top shaker. After secondary antibody incubations, the membranes were washed three times (10 min each) with TBS containing 0.05% Tween-20 at RT, and then briefly rinsed in TBS before scanning. Membranes were scanned and analyzed using an Odyssey IR scanner, running the Odyssey Imaging 3.0. software. Scans were conducted to produce medium- or high-quality images, with an intensity of 3.0–7.0 for both channels. Antibody signals were analyzed as integrated intensities of band regions in either channel.

Immunofluorescence staining

HeLa, HCT-116 and MDA-MB-231 cells were grown on coverslips and, after treatment, fixed with freshly prepared 4% paraformaldehyde for 20 min at RT or with 100% cold methanol for 10 min at −20 °C. Cells were mildly permeabilized with PBS containing 0.1% Triton and 2% bovine serum albumin at RT for 1 h. Thereafter, incubation with primary antibodies diluted in PBS with 0.1% bovine serum albumin was performed for 1 h (H3 phospho-Thr3 (JY235) monoclonal antibody, Millipore, 04–746; α-tubulin monoclonal antibody, Sigma, T6199; γ-tubulin monoclonal antibody, Sigma, T6557; anti-phospho-histone H3 (Ser10), Millipore, 06–570), washed intensively and incubated with adequate secondary antibodies labeled with Alexa 488 and Alexa 568 dyes (Molecular Probes, Invitrogen). After staining, coverslips were mounted in Mowiol (Calbiochem, Darmstadt, Germany) with DAPI (Sigma). Images were acquired using a confocal spectral Leica SP5 microscope (Leica, Milton Keynes, UK). *Z*-projection and image processing were performed using ImageJ software (Macbiophotonics, Hamilton, ON, Canada).

Chicken embryo aortic arch assay

We performed the chicken embryo aortic arch assay as described previously (Martínez *et al*., 2004). Aortic rings of ~0.8 mm length were prepared from the five aortic arches of 13-day-old chicken embryos. Each aortic ring was placed in the center of a well in a 48-well plate, covered with Matrigel and incubated with bFGF or bFGF and CHR-6494 at either 500 nM or 1.0 μM concentration, or in the presence of medium alone as a negative control. The plates were incubated at 37 °C in 5% CO_2 for 24 to 36 h, and microvessels sprouting from each aortic ring were photographed under an inverted microscope. The surface covered by the new vessels was quantified by image analysis. Six independent rings were measured per treatment. The Kruskal–Wallis test was used to identify statistically significant differences among groups.

Xenografted nude mice

Athymic *nu*/*nu* male mice (Harlam, Correzzana, Italy), aged 4–5 weeks, were used for tumor xenograft assays. Animals were maintained in a sterile environment; their cages, food and bedding were sterilized by autoclaving. The experimental design was approved by the Bellvitge Biomedical Research Institute (IDIBELL) animal facility committee. Mice were anesthetized and tumor cells were injected subcutaneously. In all, 3.5×10^6 exponentially growing HCT-116 cells diluted in 250 µl of sterile PBS were injected subcutaneously in each animal ($n = 30$). Body weight was recorded and tumor dimensions were measured twice weekly using digital calipers. Tumor volume (in mm^3) was estimated according to the formula $V = D \times d^2/2$, where D is the long axis and d the short axis of tumor. When tumors reached an average volume of 200 mm^3 (15 days after injection), 24 mice harboring homogeneous tumor sizes were randomized into two groups: (1) control group ($n = 8$) treated with vehicle (solution of 10% DMSO/20% 2-hydroxypropyl-b-cyclodextrin (Sigma-Aldrich); (2) treatment group ($n = 16$) mice was diary treated by intra-peritoneal injection of 50 mg/kg of CHR-6494 diluted in a solution of 10% DMSO/20% 2-hydroxypropyl-b-cyclodextrin in two cycles of five consecutive days for 15 days. The treatment group was randomly divided into a short-time response group ($n = 8$), defined by tumor weight at the moment of killing of the control group, and a long-time response group ($n = 8$), defined by tumor regrowth after treatment. Mice were killed at the end of treatment, and tumors from both groups were excised and weighted. The mean volume of tumor mass was expressed as mean ± s.e.m. for each mouse group, and significance was assessed by means of the Mann–Whitney *U*-test (GraphPad Prism software). Values of $P < 0.05$ were considered statistically significant. Upon killing mice, colon, lung, liver and kidney tissues were obtained to analyze endogenous toxicity by hematoxylin and eosin.

Conflict of interest

MC, DM, SP, JMcD, JO, DB, DK and SC are employees of Chroma Therapeutics.

Acknowledgements

The research leading to these results has received funding from the European Community's Sixth Framework Programme (FP6/2000-2006) under grant agreement no. LSHG-CT-2006-037415—SMARTER project, grant numbers SAF2007-00027-65134, Consolider CSD2006-49 and Dr. Josef Steiner Cancer Research Foundation. ME is an ICREA Research Professor.

References

Berdasco M, Esteller M. (2010). Aberrant epigenetic landscape in cancer: how cellular identity goes awry. *Dev Cell* **19**: 698–711.

Bryan J, Jabbour E, Prescott H, Garcia-Manero G, Issa JP, Kantarjian H. (2010). Current and future management options for myelodysplastic syndromes. *Drugs* **70**: 1381–1394.

Carpinelli P, Moll J. (2008). Aurora kinases and their inhibitors: more than one target and one drug. *Adv Exp Med Biol* **610**: 54–73.

Cheng A, Balczon R, Zuo Z, Koons JS, Walsh AH, Honkanen RE. (1998). Fostriecin-mediated G2-M-phase growth arrest correlates with abnormal centrosome replication, the formation of aberrant mitotic spindles, and the inhibition of serine/threonine protein phosphatase activity. *Cancer Res* **58**: 3611–3619.

Chopra P, Sethi G, Dastidar SG, Ray A. (2010). Polo-like kinase inhibitors: an emerging opportunity for cancer therapeutics. *Expert Opin Investig Drugs* **19**: 27–43.

Cuny GD, Robin M, Ulyanova NP, Patnaik D, Pique V, Casano G *et al*. (2010). Structure-activity relationship study of acridine analogs as haspin and DYRK2 kinase inhibitors. *Bioorg Med Chem Lett* **20**: 3491–3494.

Dai J, Sultan S, Taylor SS, Higgins JM. (2005). The kinase haspin is required for mitotic histone H3 Thr 3 phosphorylation and normal metaphase chromosome alignment. *Genes Dev* **19**: 472–488.

Dai J, Kateneva AV, Higgins JM. (2009). Studies of haspin-depleted cells reveal that spindle-pole integrity in mitosis requires chromosome cohesion. *J Cell Sci* **122**: 4168–4176.

Dai J, Sullivan BA, Higgins JM. (2006). Regulation of mitotic chromosome cohesion by Haspin and Aurora B. *Dev Cell* **11**: 741–750.

Dar AA, Goff LW, Majid S, Berlin J, El-Rifai W. (2010). Aurora kinase inhibitors–rising stars in cancer therapeutics? *Mol Cancer Ther* **9**: 268–278.

Dave SS, Fu K, Wright GW, Lam LT, Kluin P, Boerma EJ *et al*. (2006). Lymphoma/leukemia molecular profiling project. Molecular diagnosis of Burkitt's lymphoma. *N Engl J Med* **354**: 2431–2442.

D'Alise AM, Amabile G, Iovino M, Di Giorgio FP, Bartiromo M, Sessa F *et al*. (2008). Reversine, a novel Aurora kinases inhibitor, inhibits colony formation of human acute myeloid leukemia cells. *Mol Cancer Ther* **7**: 1140–1149.

Eswaran J, Patnaik D, Filippakopoulos P, Wang F, Stein RL, Murray JW *et al*. (2009). Structure and functional characterization of the atypical human kinase haspin. *Proc Natl Acad Sci USA* **106**: 20198–20203.

Folkman J. (2007). Angiogenesis: an organizing principle for drug discovery? *Nat Rev Drug Discov* **6**: 273–286.

Girdler F, Gascoigne KE, Eyers PA, Hartmuth S, Crafter C, Foote KM *et al*. (2006). Validating Aurora B as an anti-cancer drug target. *J Cell Sci* **119**: 3664–3675.

Gleixner KV, Ferenc V, Peter B, Gruze A, Meyer RA, Hadzijusufovic E *et al*. (2010). Polo-like kinase 1 (Plk1) as a novel drug target in chronic myeloid leukemia: overriding imatinib resistance with the Plk1 inhibitor BI 2536. *Cancer Res* **70**: 1513–1523.

Götze K, Platzbecker U, Giagounidis A, Haase D, Lübbert M, Aul C *et al*. (2010). Azacitidine for treatment of patients with myelodysplastic syndromes (MDS): practical recommendations of the German MDS Study Group. *Ann Hematol* **89**: 841–850.

Graham JS, Kaye SB, Brown R. (2009). The promises and pitfalls of epigenetic therapies in solid tumours. *Eur J Cancer* **45**: 1129–1136.

Harrington EA, Bebbington D, Moore J, Rasmussen RK, Ajose-Adeogun AO, Nakayama T *et al*. (2004). VX-680, a potent and selective small-molecule inhibitor of the Aurora kinases, suppresses tumor growth *in vivo*. *Nat Med* **10**: 262–267.

Higgins JM. (2001). Haspin-like proteins: a new family of evolutionarily conserved putative eukaryotic protein kinases. *Protein Sci* **10**: 1677–1684.

Johnson EF, Stewart KD, Woods KW, Giranda VL, Luo Y. (2007). Pharmacological and functional comparison of the polo-like kinase family: insight into inhibitor and substrate specificity. *Biochemistry* **46**: 9551–9563.

Jones PA, Baylin SB. (2007). The epigenomics of cancer. *Cell* **128**: 683–692.

Kelly AE, Ghenoiu C, Xue JZ, Zierhut C, Kimura H, Funabiki H. (2010). Survivin reads phosphorylated histone H3 threonine 3 to activate the mitotic kinase Aurora B. *Science* **330**: 235–239.

Kim MS, Kwon HJ, Lee YM, Baek JH, Jang JE, Lee SW *et al*. (2001). Histone deacetylases induce angiogenesis by negative regulation of tumor suppressor genes. *Nat Med* **7**: 437–443.

Kouzarides T. (2007). Chromatin modifications and their function. *Cell* **128**: 693–705.

Lane AA, Chabner BA. (2009). Histone deacetylase inhibitors in cancer therapy. *J Clin Oncol* **27**: 5459–5468.

Malumbres M, Pevarello P, Barbacid M, Bischoff JR. (2008). CDK inhibitors in cancer therapy: what is next? *Trends Pharmacol Sci* **29**: 16–21.

Macurek L, Lindqvist A, Medema RH. (2009). Aurora-A and hBora join the game of Polo. *Cancer Res* **69**: 4555–4558.

Marks PA. (2010). Histone deacetylase inhibitors: a chemical genetics approach to understanding cellular functions. *Biochim Biophys Acta* **1799**: 717–725.

Martínez A, Zudaire E, Portal-Núñez S, Guédez L, Libutti SK, Stetler-Stevenson WG *et al*. (2004). Proadrenomedullin N-terminal 20 peptide is a potent angiogenic factor and its inhibition results in reduction of tumor growth. *Cancer Res* **64**: 6489–6494.

Ma X, Ezzeldin HH, Diasio RB. (2009). Histone deacetylase inhibitors: current status and overview of recent clinical trials. *Drugs* **69**: 1911–1934.

Musacchio A, Salmon ED. (2007). The spindle-assembly checkpoint in space and time. *Nat Rev Mol Cell Biol* **8**: 379–393.

Nakai R, Lida S, Takahashi T, Tsujita T, Okamoto S, Takada C *et al*. (2009). K858, a novel inhibitor of mitotic kinesin Eg5 and antitumor agent, induces cell death in cancer cells. *Cancer Res* **69**: 3901–3909.

Nilsson J, Yekezare M, Minshull J, Pines J. (2008). The APC/C maintains the spindle assembly checkpoint by targeting Cdc20 for destruction. *Nat Cell Biol* **10**: 1411–1420.

Oke A, Pearce D, Wilkinson RW, Crafter C, Odedra R, Cavenagh J *et al*. (2009). AZD1152 rapidly and negatively affects the growth and survival of human acute myeloid leukemia cells *in vitro* and *in vivo*. *Cancer Res* **69**: 4150–4158.

Patnaik D, Jun Xian, Glicksman MA, Cuny GD, Stein RL, Higgins JM. (2008). Identification of small molecule inhibitors of the mitotic kinase haspin by high-throughput screening using a homogeneous time-resolved fluorescence resonance energy transfer assay. *J Biomol Screen* **13**: 1025–1034.

Rebacz B, Larsen TO, Clausen MH, Rønnest MH, Löffler H, Ho AD *et al*. (2007). Identification of griseofulvin as an inhibitor of centrosomal clustering in a phenotype-based screen. *Cancer Res* **67**: 6342–6350.

Rosasco-Nitcher SE, Lan W, Khorasanizadeh S, Stukenberg PT. (2008). Centromeric Aurora-B activation requires TD-60, microtubules, and substrate priming phosphorylation. *Science* **319**: 469–472.

Rosenwald A, Alizadeh AA, Widhopf G, Simon R, Davis RE, Yu X *et al*. (2001). Relation of gene expression phenotype to immunoglobulin mutation genotype in B cell chronic lymphocytic leukemia. *J Exp Med* **194**: 1639–1647.

Stemmann O, Gorr IH, Boos D. (2006). Anaphase topsy-turvy: Cdk1 a securin, separase a CKI. *Cell Cycle* **5**: 11–13.

Takeuchi T, Takahashi N, Ishi K, Kusayanagi T, Kuramochi K, Sugawara F. (2009). Antitumor antibiotic fostriecin covalently binds to cysteine-269 residue of protein phosphatase 2A catalytic subunit in mammalian cells. *Bioorg Med Chem* **17**: 8113–8122.

Tao Y, Leteur C, Calderaro J, Girdler F, Zhang P, Frascogna V *et al*. (2009). The aurora B kinase inhibitor AZD1152 sensitizes cancer cells to fractionated irradiation and induces mitotic catastrophe. *Cell Cycle* **8**: 3172–3181.

Thompson SL, Bakhoum SF, Compton DA. (2010). Mechanisms of chromosomal instability. *Curr Biol* **20**: R285–R295.

Vassilev LT, Tovar C, Chen S, Knezevic D, Zhao X, Sun H *et al*. (2006). Selective small-molecule inhibitor reveals critical mitotic functions of human CDK1. *Proc Natl Acad Sci USA* **103**: 10660–10665.

Villa F, Capasso P, Tortorici M, Forneris F, de Marco A, Mattevi A *et al*. (2009). Crystal structure of the catalytic domain of Haspin, an atypical kinase implicated in chromatin organization. *Proc Natl Acad Sci USA* **106**: 20204–20209.

Wang F, Dai J, Daum JR, Niedzialkowska E, Banerjee B, Stukenberg PT *et al*. (2010). Histone H3 Thr-3 phosphorylation by Haspin positions Aurora B at centromeres in mitosis. *Science* **330**: 231–235.

Yamagishi Y, Honda T, Tanno Y, Watanabe Y. (2010). Two histone marks establish the inner centromere and chromosome bi-orientation. *Science* **330**: 239–243.

Zubia A, Ropero S, Otaegui D, Ballestar E, Fraga MF, Boix-Chornet M *et al*. (2009). Identification of (1H)-pyrroles as histone deacetylase inhibitors with antitumoral activity. *Oncogene* **28**: 1477–1484.

Supplementary Information accompanies the paper on the Oncogene website (http://www.nature.com/onc)